Proceedings of the 7th World Congress on Momentum, Heat and Mass Transfer (MHMT'22)
Lisbon, Portugal – April 10 – 12, 2022
Paper No. ENFHT 198 (The number assigned by the OpenConf System)
DOI: TBA

Non-Newtonian Spreading Simulation of Molten Nuclear Combustible

Thomas Schiano[1,2], Barbara Bigot[1], Jean-François Haquet[1], Pierre Saramito[2], Claude Smutek[3]
[1]CEA, DES/IRESNE/DTN/SMTA/LMAG
Cadarache, Saint-Paul-lez-Durance, France, thomas.schiano@cea.fr
[2]Lab. J. Kuntzmann, CNRS and Grenoble Alpes University
700 Avenue Centrale, Saint Martin d'Hères, France
[3]Lab. Géosciences Réunions, Réunion University, Institut de Physique du Globe de Paris
15 Avenue René Cassin, Saint Denis

Abstract - In this paper, the non-dimensional 3D model for a free-surface non-Newtonian anisotherm flow is described. Its use for molten nuclear reactor core (corium) in the event of severe accidents is argued using similarity criteria. The model is then implemented in a finite element code based on the C++ library Rheolef. The resulting simulations are compared to experimental data from the prototypical corium spreading experiment VEU7.

Keywords**:** Viscoplastic Fluid, Spreading, Corium, Severe Nuclear Accidents, Simulation, Free Surface Flow

1. Introduction

During a hypothetical nuclear reactor severe accident the reactor core would melt fully or partially to form a mixture of nuclear combustible, its rod and assembly, in a metallic or oxidized form, called corium. Part of the Ex-Vessel Retention (EVR) strategy for the European Pressurized Reactor (EPR) concept [1] is to dedicate a section of the reactor to the melt spreading on a concrete basemat, to reduce surface heat load due to radioactive heat decay on the structure.

Prototypic corium spreading experiments such as the VULCANO tests [2] provide valuable experimental data on the laminar part of the spreading process, to check the validity of safety codes.

Current industrial corium spreading codes include THEMA [3] and CORFLOW [4] that use a regularized Binghamian description of the fluid. The viscoplastic corium description has been gathering interest in order to obtain a more accurate description of the stopping process and length, since the viscosity and yield stress measurements made by Roche et al. [5].

As pointed out by Saramito and Wachs [6], the regularization approach currently used in industrial codes lacks a general convergence result of the solution with the regularization parameter and cannot follow the unyielded regions of a yield stress fluid flow where the deformation rate tensor is equal to zero.

Here, we propose a non-regularized 3D height-averaged finite element approach. It has been described and simulated successfully for lava flows by Bernabeu et al. [7] using the finite element library Rheolef [8]. A second-order temperature polynomial approximation in the vertical direction is used with varying viscosity using the Shaw model [9].

2. Methods

The study domain Ω is defined as the sum of the melt domain $\Omega_f(t)$, substrate domain Ω_s and environment $\Omega_a(t)$ as described on Fig.1. The non-dimensional mass, momentum along x and z axes and energy conservation equations read:

$$\partial_x u_x + \partial_y u_y + \partial_z u_z = 0, \quad (1)$$

with, u_x, u_y and u_z the components of velocity,

$$\varepsilon^2 Re(\partial_t u_x + u_x \partial_x u_x + u_y \partial_y u_x + u_z \partial_z u_x) = -\partial_x p + \varepsilon^2(\partial_x \tau_{xx} + \partial_y \tau_{xy}) + \partial_z \tau_{xz}, \quad (2)$$

$$\varepsilon^4 Re(\partial_t u_z + u_x \partial_x u_z + u_y \partial_y u_z + u_z \partial_z u_z) = 1 - \partial_z p + \varepsilon^2(\partial_x \tau_{zx} + \partial_y \tau_{zy} + \partial_z \tau_{zz}), \quad (3)$$

with ε=H/L the aspect ratio of the characteristic height to the characteristic length, p the pressure, τ the deviatoric part of the Cauchy stress tensor and Re the Reynolds number. The momentum equation along the y-axis is similar, thus we do not give it here.

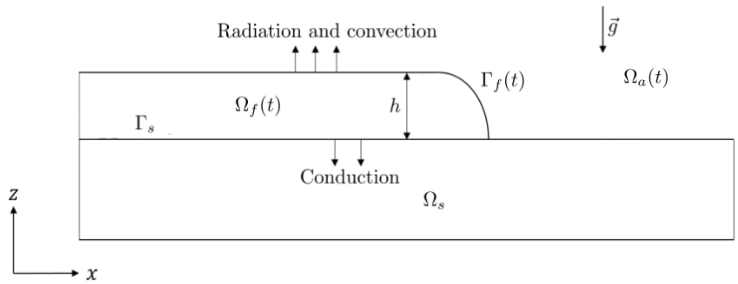

Fig. 1: Corium spreading principle and domain definition diagram

$$\partial_t\theta u_x\partial_x\theta + u_y\partial_y\theta + u_z\partial_z\theta = \frac{1}{Pe}\left(\varepsilon^2\partial_{xx}\theta + \varepsilon^2\partial_{yy}\theta + \partial_{zz}\theta + \frac{Br}{2}\varepsilon^2\left(\sum_{\alpha,\beta}\tau_{\alpha\beta}\dot{\gamma}_{\alpha\beta} + \varepsilon^2\tau_{zz}\dot{\gamma}_{zz} + \sum_{\alpha}\tau_{\alpha z}\dot{\gamma}_{\alpha z}\right)\right). \quad (4)$$

with θ the temperature, $\dot{\gamma}$ the strain rate tensor, Pe the Péclet number and Br the Brinkman number. The conservation equations are completed by the non-dimensional Herschel-Bulkley model:

$$\begin{cases} \tau = \left(\frac{Bi\,\tau_y(\theta)}{E} + K(\theta)E^{n-1}\right)\dot{\gamma},\ if\ \ E \neq 0, \\ T \leq Bi\tau_y(\theta), otherwise. \end{cases} \quad (5)$$

with $K(\theta)$ the temperature dependent consistency index, τ_y the temperature dependent yield stress, n the fluid index, Bi the Bingham number, $T = \varepsilon|\tau|$ and $E = \varepsilon|\dot{\gamma}|$. The consistency index is equivalent to a viscosity when $n = 1$ for the Bingham model. The temperature evolution of both $K(\theta)$ and $\tau_y(\theta)$ follow a model as described by Shaw for lava [9], for example for consistency $K(\theta) = K_0 e^{Arr(\theta_e - \theta)}$ with K_0 the consistency at θ_e the initial melt temperature and Arr the Shaw model coefficient.

The free surface is described by the equation $\partial_t\varphi + u \cdot \nabla\varphi = 0$ with $\varphi = z - h$ the level-set function and h the flow height. Those equations are completed by constant initial conditions for velocity, height and temperature, Dirichlet boundary conditions for velocity and inlet temperature and a free-surface condition at $\Gamma_f(t)$. Heat transfer at the free surface includes radiation and convection:

$$-\varepsilon^2\left(\partial_x h\partial_x\theta + \partial_y h\partial_y\theta\right) + \partial_z\theta + Rp_\mu(\theta)\theta + Nu\theta = 0 \ \ on\ \Gamma_f(t), \quad (6)$$

with R a non-dimensional radiation number, Nu the Nusselt number and p_ξ a third order polynomial with coefficients dependent on $\xi = \frac{\theta_a}{\theta_e - \theta_a}$ a temperature ratio number. Heat transfer with the substrate is mainly conductive, with k and k_s respectively the melt and substrate temperature conduction coefficients:

$$\varepsilon^2\left(\partial_x h\partial_x\theta + \partial_y h\partial_y\theta\right) - \partial_z\theta = -\frac{k_s}{k}\left(\varepsilon^2\left(\partial_x h\partial_x\theta_s + \partial_y h\partial_y\theta_s\right) - \partial_z\theta_s\right)\ on\ \Gamma_s, \quad (7)$$

Heat conduction in the semi-infinite substrate is approached using the formula by Carslaw and Jaeger [10] p.60, with Fo the Fourier number:

$$\theta_s(z,t) = \theta(x,y,z=0,t)\mathrm{erfc}\left(\frac{-z\sqrt{Fo}}{2\sqrt{t}}\right)\ in\ \Omega_s. \quad (8)$$

The dimensionless numbers from this set of equations are computed for both a lava eruption of the Piton de la Fournaise volcano in 2010 [9,11] and the VEU7 spreading experiment [2,5], using their properties at their initial temperature, respectively $1423\ K$ and $2450\ K$ for lava and corium. The resulting numbers show regime similarities for both flows, mainly as they are both laminar, with radiative heat transfer at the free surface and can be considered viscoplastic.

Table 1: Dimensionless numbers computed using data from measurements on 2010 Piton de la Fournaise eruption and VEU7 corium spreading test. The eruption temperature for lava is $1423\ K$ and that of corium at the inlet is $2450\ K$.

Similarity criterion	Definitions	Lava	Corium
Reynolds number Re	$Re = \frac{\rho U L}{\mu}$ with ρ the density, U and μ the characteristic velocity and dynamic viscosity	$4.75\ 10^{-1}$	$1.40\ 10^{1}$
Bingham number Bi	$Bi = \frac{\tau_{y,0} L}{\mu U}$ with $\tau_{y,0}$ the initial yield stress	4.63	$1.89\ 10^{-1}$
Péclet number Pe	$Pe = \frac{\rho c_p U L}{k}$ with c_p the specific heat capacity	$2.91\ 10^{6}$	$1.04\ 10^{6}$
Brinkman number Br	$Br = \frac{U^2 \mu}{k(\theta_e - \theta_a)}$ with θ_a the ambient temperature	$2.08\ 10^{-5}$	$1.25\ 10^{-2}$
Stanton number St	$St = \frac{Nu}{Pe} = \frac{\lambda}{\rho U c_p}$ with λ the convective heat transfer coefficient	$1.37\ 10^{-5}$	$1.85\ 10^{-4}$
Radiation number R	$R = \frac{\epsilon \sigma_{SB} (\theta_e - \theta_a)^3 L}{k}$ with ϵ the emissivity and σ_{SB} the Stefan-Boltzmann constant.	$3.78\ 10^{1}$	$2.70\ 10^{1}$

The precedent equations are then reduced at the order 0 in ε by making the hypothesis that the aspect ratio $\varepsilon = 0.15$ for the VEU7 experiment is small and then vertically-averaged. The problem becomes height and temperature dependent only, as the other unknowns can be deduced from them. This non-dimensional vertical averaged problem is then implemented using the C++ mesh adaptive finite element library Rheolef [8].

3. Results and Discussion

Simulations have been ran for different value of Fourier number, corresponding to property materials of the ceramic and concrete substrate given in the VEU7 benchmark by Journeau et al. [2]. The results in terms of spreading length are given on Fig. 2, showing good agreement between the simulation and experimental results for the concrete substrate in terms of dynamics and final length, though the ceramic substrate show greater discrepancies. This can be partially explained by the use of two connected channels in the experiment while only one was represented in the simulation, preventing backflow from one channel to the other from happening numerically.

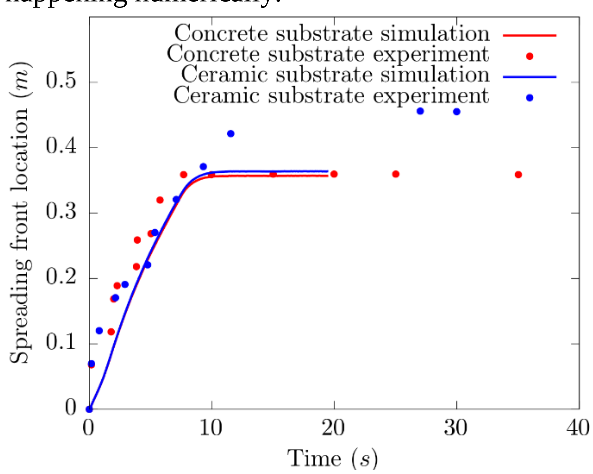

Fig. 2: Melt front evolution through time, comparison between experimental data from the VEU7 experiment and simulation.

The evolution of temperature in the concrete substrate is of interest, as it is a criteria for its degassing and ablation, and ultimately its integrity is the condition of success of the EVR strategy. The results obtained from using eq. (8) show generally good agreement with the measurements from thermocouples. The main differences between experimental and simulation data are found for the thermocouple located at $z = -2 \pm 1.5\ mm$, due to the large uncertainties on its depth and the potential degassing that occurs for the higher temperatures it reaches.

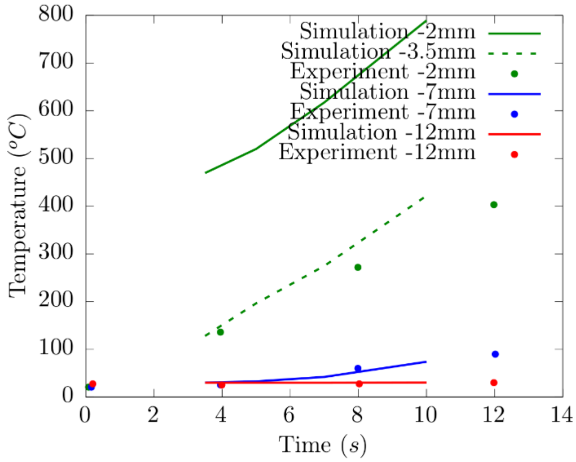

Fig. 3: Concrete substrate temperature evolution for the VEU7 experiment and its simulation, for thermocouples at $x = 12\ cm$ and $z = -2, -7, -12 mm$.

4. Conclusion

The viscoplastic simulation of corium spreading shows interesting results in terms of spreading length, time and substrate temperature evolution. Realizing a two channels simulation could provide greater validation of the model compared to the VEU7 experiment. Adding degassing of the substrate and its ablation might give greater insight on the EVR strategy for nuclear power plants severe accidents management.

References

[1] H. A. Weisshäupl, « Severe accident mitigation concept of the EPR », *Nuclear Engineering and Design*, vol. 187, nº 1, p. 35-45, jan. 1999, doi.org/10.1016/S0029-5493(98)00256-8.

[2] C. Journeau, J.-F. Haquet, B. Spindler, C. Spengler, et J. Foit, « The VULCANO VE-U7 Corium spreading benchmark », *Progress in Nuclear Energy*, vol. 48, nº 3, p. 215-234, apr. 2006, doi.org/10.1016/j.pnucene.2005.09.009.

[3] B. Spindler and J. M. Veteau, « The simulation of melt spreading with THEMA code », *Nuclear Engineering and Design*, vol. 236, nº 4, p. 425-441, févr. 2006, doi.org/10.1016/j.nucengdes.2005.09.016.

[4] R. Wittmaack, « Simulation of Free-Surface Flows with Heat Transfer and Phase Transitions and Application to Corium Spreading in the EPR », *Nuclear Technology*, vol. 137, nº 3, p. 194-212, 2002, doi.org/10.13182/NT02-A3268.

[5] M. F. Roche, D. V. Steidl, L. Leibowitz, J. K. Fink, et B. Raj Sehgal, « Viscosity of Corium-Concrete Mixtures at High Temperatures. », Argonne National Laboratory, ANL Report ACE-TR-C37, 1994.

[6] P. Saramito and A. Wachs, « Progress in numerical simulation of yield stress fluid flows », *Rheol Acta*, vol. 56, nº 3, p. 211-230, mars 2017, doi.org/10.1007/s00397-016-0985-9.

[7] N. Bernabeu, P. Saramito, et C. Smutek, « Modelling lava flow advance using a shallow-depth approximation for three-dimensional cooling of viscoplastic flows », *Geological Society, London, Special Publications*, vol. 426, nº 1, p. 409-423, 2016, doi.org/10.1144/SP426.27.

[8] P. Saramito, « Rheolef 7.1, an efficient C++ finite element environment », *Rheolef 7.1, an efficient C++ finite element environment*, 2019.https://www-ljk.imag.fr/membres/Pierre.Saramito/rheolef (consulted 06/11/2019).

[9] H. R. Shaw, « Rheology of Basalt in the Melting Range », *Journal of Petrology*, vol. 10, nº 3, p. 510-535, oct. 1969, doi.org/10.1093/petrology/10.3.510.

[10] H. S. Carslaw and J. C. Jaeger, *Conduction of Heat in Solids*, 2nd ed. USA: Oxford University Press, 1959 p.60.

[11] N. Villeneuve, D. R. Neuville, P. Boivin, P. Bachèlery, et P. Richet, « Magma crystallization and viscosity: A study of molten basalts from the Piton de la Fournaise volcano (La Réunion island) », *Chemical Geology*, vol. 256, nº 3-4, p. 242-251, nov. 2008, doi.org/10.1016/j.chemgeo.2008.06.039.